Nanoscale Studies of Cuprate Superconductors in the Current-Carrying State

J. Y.T. Wei, J. Ngai and P. Morales

University of Toronto, Department of Physics, 60 St. George Street, Toronto, ON, M5S1A7 Canada

ABSTRACT

We present a new class of nanoscale experiments on cuprate superconductors in the current-carrying state. These experiments are aimed at studying how the high-T_c order parameter responds, in both real and reciprocal space, when driven by a sizable phase gradient. First, scanning tunneling spectroscopy was performed on current-carrying $YBa_2Cu_3O_{6+x}$ (YBCO) thin-film strips, to reveal a remarkable suppression of the low-energy Andreev states indicating an increase in the local phase fluctuations. Second, transport measurements were made on optimally-doped YBCO nanostructures, to show anomalous current-voltage nonlinearities consistent with the formation of current-driven phase slip lines. These results are discussed in the general context of non-rigidity of the high-T_c order parameter under electrodynamic perturbation.

Keywords: High-T_c, superconductivity, cuprates, STM, thin-film, nanostructures, d-wave, order parameter, fluctuations, phase slips.

1. INTRODUCTION

Superconductors are well known for their ability to carry current without dissipation, thanks to the macroscopic phase coherence among paired electrons. In reduced dimensions, where fluctuation effects can become pronounced, the loss of phase coherence and the appearance of dissipation under an applied current are physical issues of both fundamental interest and technological importance. For conventional superconductors, these issues have been well studied experimentally, through the phenomenology of vortex-antivortex unbinding in 2D[1, 2] and phase slips in 1D.[3, 4] For the high-T_c cuprate superconductors, on the other hand, similar studies have not been in abundance, limited largely by the complex chemistry and short coherence lengths of these oxide materials.[5] Nevertheless, it is believed that high-T_c superconductors are inherently fragile against phase fluctuations by virtue of their low superfluid densities.[6] Considering all these factors, it would be very revealing to probe the short-range phase dynamics of cuprate superconductors in the current-carrying state.

This paper presents a new class of nanoscale experiments designed to study how the high-T_c order parameter responds, in both real and reciprocal space, to the phase gradient carried by a supercurrent. Section 2 reports on a novel scanning tunneling spectroscopy (STS) study of current-carrying $YBa_2Cu_3O_{6+x}$ (YBCO) thin films. Section 3 reports on electrical transport measurements of YBCO microwires which were nanofabricated by a chemical-free method. In these experiments, we have observed several new phenomena related to either phase fluctuations or phase slippage, both driven by the applied current. These remarkable phenonmena could be interpreted as manifestations of *non-rigidity* of the high-T_c order parameter under electrodynamic perturbation.

2. STS ON CURRENT-CARRYING YBCO THIN FILMS

High-T_c cuprate superconductors are distinguished by their low carrier densities and short coherence lengths. These properties imply an inherently low superfluid stiffness, making the superconducting order parameter (OP) prone to fluctuations in its phase.[6] Such phase fluctuations, when thermally-driven, could weaken the superconducting phase coherence while maintaining finite pairing amplitude.[7] This "pairing-without-condensation" scenario has in fact been invoked to explain the well-known pseudogap phenomenon,[8] in relation to the notion of incoherent bosonized pairs.[9] However, despite the wealth of experimental data indicating the presence of phase fluctuations in the cuprates, there has also been much inconclusive and even contrary evidence.[10] One of the key experimental limitations to clarifying this issue has been the high temperatures or magnetic fields needed to

Strongly Correlated Electron Materials: Physics and Nanoengineering, edited by Ivan Bozovic, Davor Pavuna, Proceedings of SPIE Vol. 5932 (SPIE, Bellingham, WA, 2005) · 0277-786X/05/$15 · doi: 10.1117/12.631743

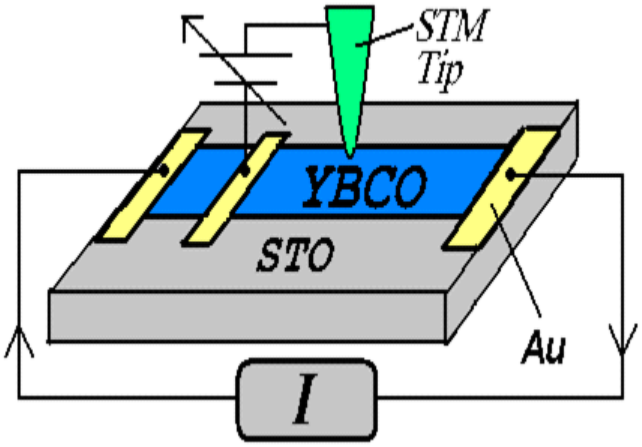

Figure 1. Schematic of our experimental set-up showing an STM tip over a YBCO thin-film strip grown on an STO substrate. The tip is biased relative to the sample by a gold pad on the sample surface. Spectroscopy measurements are made while a simultaneous current is passed through the film strip.

produce pseudogap conditions *thermodynamically*. Another challenge for directly observing the effects of phase fluctuations is to probe both the OP phase and amplitude within the very short (∼nm) coherence-length scale.

We have developed a novel scanning tunneling spectroscopy (STS) technique to study $YBa_2Cu_3O_{6+x}$ (YBCO) thin-film strips carrying an applied current at 4.2K. This directly-applied supercurrent acts as a phase gradient to *electrodynamically*, rather than *thermodynamically*, perturb the superconducting OP. It is now well established that tunneling into a *d*-wave superconductor involves both quasiparticle transmission and Andreev reflection, with sensitivity to both the phase and amplitude of the pair wavefunction.[11–14] By virtue of its nanoscale junction size, STS can thus provide coherence-length scale information on how the OP evolves when driven by an applied supercurrent. In our experiment we find that the *phase*-sensitive spectral features are systematically suppressed while the *amplitude*-dependent features remain largely unchanged. These observations indicate that a supercurrent can weaken the *local* phase coherence while preserving the pairing amplitude in YBCO, suggesting that phase fluctuations do play a significant role in high-temperature superconductivity.

2.1. STS Experimental

Figure 1 shows a schematic of our experimental STS setup, with a Pt-Ir tip positioned over a YBCO thin-film strip and a Au contact providing the bias voltage V between tip and sample. STS is performed by measuring the tunneling current I_t as a function of the bias voltage, while a simultaneous current I_s is applied through the superconducting film at 4.2K. The I_s is supplied from a current source below, through Au contacts on the ends of the film strip. The special floating-ground current source along with the high tunnel junction impededance (∼0.1GΩ) ensures that I_t (∼1nA) is decoupled from I_s (∼100mA). A special circuitry is used to synchronize I_s with the STS data acquisition.[15] Short duty-cycle I_s pulses ≈200μs in duration are used to prevent sample Joule heating, which could occur at high current levels. For our experiment, this versatile STS technique enabled highly reproducible tunneling I-V measurements at nanometer length scales.

For our experiment, pulsed laser-ablated deposition (PLD) was used to grow the YBCO thin-film strips on $SrTiO_3$ (STO) substrates.[16] Both {110} and {001} oriented films were made, the former using a templating technique involving a $PrBa_2Cu_3O_7$ underlayer. The films were typically 50nm thick and in a 1mm x 3mm strip-line geometry, aligned along <100> and $[1\bar{1}0]$ respectively for the {001} and {110} films. The films showed critical temperatures of (T_c≈87K) and transport critical-current densities of (J_c≈5×10^{6}A/cm^2) at 4.2K. Epitaxiality of the films was confirmed by x-ray diffraction and rocking-curve analysis. Film surface quality was determined

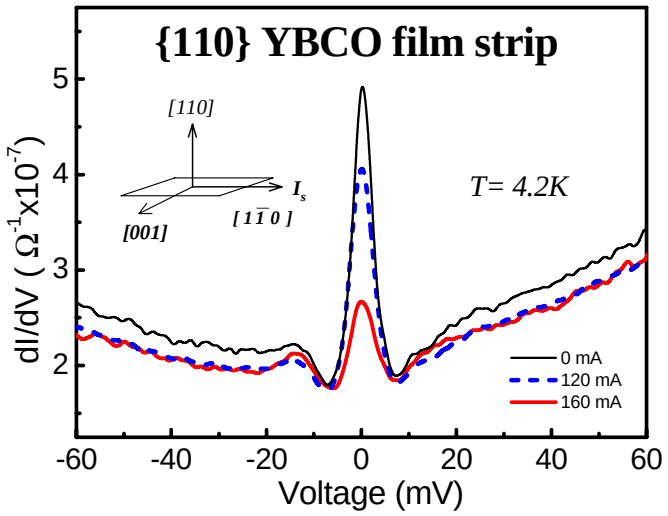

Figure 2. dI/dV spectra obtained on a {110} YBCO film strip carrying a supercurrent applied along [1$\bar{1}$0] at 4.2K.

directly from topography measurements using our STS setup. Shown in the inset of Figure 5 is a topographic image taken on a {001} film, indicating smooth terraces with large c-axis faces ∼100nm in size and ab-plane edges ∼3nm in height.

2.2. STS Data

Figure 2 shows tunneling conductance data taken at 4.2K on a {110} film strip at various current levels applied along [1$\bar{1}$0]. The dI/dV spectra were obtained through numerical differentiation of the measured I-V data. These spectra show a well-developed zero-bias conductance peak (ZBCP) structure which is suppressed in height but only slightly changed in width by the applied current. These ZBCP structures have been commonly observed in tunneling experiments on YBCO, and could be identified as the low-energy Andreev states based on a predominant d-wave OP.[11–13] The low-energy states arise from the interference between *consecutive* Andreev-reflected quasielectrons and quasiholes in high-impedance, specular junctions oriented normal to a non-principle axis (see right inset in Fig.3). The time-reversed quasiparticles interfere constructively by virtue of the phase sign change of the d-wave OP about its nodal (k_x=±k_y) axes.[11] As will be shown in the spectral analysis below, this interference process renders the low-energy Andreev states inherently sensitive to OP phase fluctuations.

Two features of the ZBCP spectral evolution are noteworthy. First, the ZBCP does not appear to split, indicating time-reversal invariance of the d-wave OP in our near-optimally doped YBCO samples at 4.2K up to 160mA the maximum current level applied. Second, the area under dI/dV is clearly not conserved, indicating negligible thermal broadening with a loss of Andreev states. The non-splitting of the ZBCP we observed is quantitatively consistent with a recent theoretical calculation[17] which shows no Doppler shift[18] of the Andreev-bound states in this geometry until a much higher supercurrent density. However, the clear loss of Andreev states we observed was not anticipated by this mean-field calculation.

2.3. Phase Fluctuation Analysis

To understand the observed suppression of low-energy Andreev states, we introduce a phase fluctuation model using the generalized Blonder-Tinkham-Klapwijk (BTK) formalism for tunneling into a d-wave superconductor.[11–13] The generalized BTK expression for tunneling conductance G_{ns} is given by:

$$\frac{G_{ns}}{G_{nn}} = \int_{-\frac{\pi}{2}}^{+\frac{\pi}{2}} d\theta \int_{-\infty}^{+\infty} dE[1+|a|^2-|b|^2]\frac{\partial f(E-eV)}{\partial V} \quad (1)$$

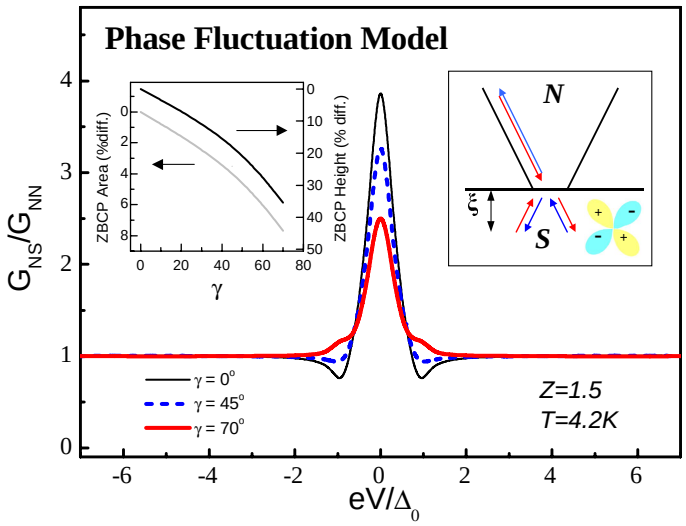

Figure 3. Phase fluctuation model showing the evolution of the ZBCP on a {110} junction as a function of the phase smearing parameter γ. Left inset shows the ZBCP height and spectral area as a function of γ. Right inset illustrates the Andreev interference process based on the d-wave phase sign change.

Here, a and b are the Andreev-reflection and normal-reflection coeffiecients, f is the Fermi-Dirac function, G_{nn} is the normal-state junction conductance, E the quasiparticle energy, and θ the polar angle in k-space. To model the effects of OP phase fluctuations, we modify the BTK kernel by adding a phase factor $e^{i\varphi}$ to the phase-interference term in its denominator (see Eqn.2 below) then integrating it over the domain of phase φ weighted by a Gaussian of width γ:

$$1+|a|^2-|b|^2=\int_{-\pi}^{+\pi}d\varphi\frac{1}{\sqrt{2\pi\gamma}}e^{-\varphi^2/\gamma^2}\times \frac{16(1+|\Gamma_+|^2)\cos^4\theta+4Z^2(1-|\Gamma_+\Gamma_-|^2)\cos^2\theta}{|4\cos^2\theta+Z^2[1-\Gamma_+\Gamma_-e^{i\phi_--i\phi_++i\varphi}]|^2} \tag{2}$$

The amplitude factors $\Gamma_\pm=(E/|\Delta_\pm|)-\sqrt{(E/|\Delta_\pm|)^2-1}$ contain a d-wave gap function using a gap maximum denoted by Δ_0. The phase factors $e^{i\phi_\pm}=\Delta_\pm/|\Delta_\pm|$ represent the sign of the pair potential $\Delta_\pm=\Delta(\theta_\pm)$ which is experienced by an Andreev-reflected quasielectron (or quasihole) propagating at an angle θ_+ (or $\theta_-=\pi-\theta_+$) relative to the junction normal (see right inset in Fig.3). Through the extra phase introduced by $e^{i\varphi}$, the weighted integral over φ essentially smears out the *relative* phase between *consecutive* Andreev-reflected quasiparticles. Our phenomenological approach can be compared with the more rigorous treatment of Reference 19 which uses a 2D X-Y model based on vortex fluctuations.[20]

The results of our phase fluctuation model for a {110} junction are shown in Figure 3, plotted as normalized conductance G_{ns}/G_{nn}. Our simulations used a typical gap maximum of Δ_0=15meV, along with a large barrier parameter Z=1.5, and temperature of T=4.2K to model our experimental conditions. A clear trend of ZBCP suppression is seen versus the phase-smearing parameter γ, showing a drop in the peak height and a loss of spectral area. Detailed evolutions of height and area versus γ are plotted in the left inset of Fig.3. Comparing our data in Fig.2 with the simulations in Figure 3, it is clear that the ZBCP suppression could be qualitatively attributed to the *dephasing* effects of OP phase fluctuations. Physically speaking, consecutive Andreev-reflected quasiparticles which are bound within a coherence length ξ from the specular {110} surface (see right inset of Fig.3) would experience an effective smearing in their relative phase as a result of the phase fluctuations, thus interfering less constructively. This phase smearing leads directly to a loss in the low-energy Andreev states, resulting in the ZBCP suppression seen in the data. It should be noted that low-energy Andreev states could

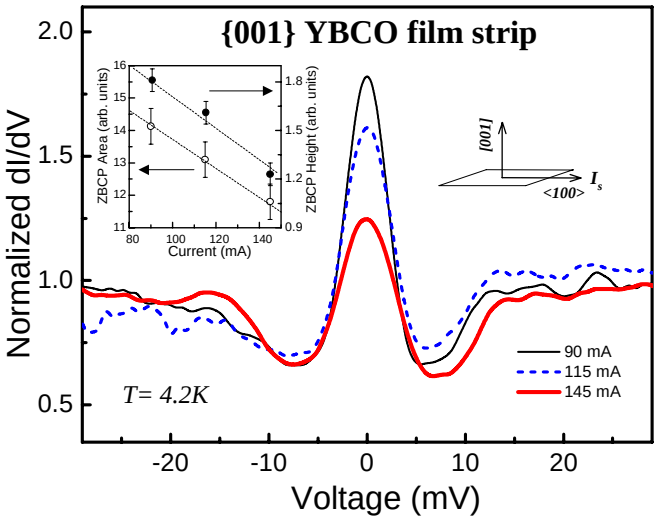

Figure 4. Normalized dI/dV spectra obtained on a {001} YBCO thin-film strip carrying a supercurrent applied predominantly along <100> at 4.2K. Left inset shows the evolution of the ZBCP height and spectral area versus the applied current.

also form under *non-specular* conditions in a d-wave superconductor, i.e. near grain boundaries, extended non-magnetic impurities, or surface interstitial defects.[21–27] Like the specular Andreev-bound states, nevertheless, these low-energy resonance states are essentially also based on d-wave Andreev interference, which should render them similarly sensitive to local phase fluctuations. A detailed theoretical study would be needed to address these non-specular scenarios.

2.4. Results and Discussion

Although the phase fluctuation model given above can provide a phenomenological description of the spectral suppression observed, it would be important to know the physical mechanism by which the applied supercurrent is driving the phase fluctuations. Here we speculate on some plausible scenarios. One possibility would be the proliferation of thermally-generated vortex-antivortex pairs, in a Kosterlitz-Thouless type scenario,[28,29] but with current providing an additional unbinding force.[1,2] Another possibility may involve direct interactions between the supercurrent and fluctuating spin/charge stripes,[30–32] perhaps in a manner similar to phase-slip processes which have been seen in transport studies[33,34] and will be discussed in Section 3. In principle, the *static* phase gradient carried by the supercurrent could also couple *dynamically* with other types of phase-ordered states, such as spin-density waves,[35] staggered flux-like states[36,37] or collective modes,[38,39] to produce enhanced phase fluctuations. Recent theoretical work has focused on how the d-wave Andreev-bound states and quasiparticle density of states could evolve under an applied supercurrent.[17,40] In this regard, it should be emphasized that our analysis of the suppression of low-energy Andreev states is based on a non-rigid OP with respect to phase fluctuations. Other forms of OP non-rigidity are also possible, for example with respect to changes in the pairing symmetry.[41,42] Phase-sensitive experiments have indicated the d-wave pairing symmetry to be robust under doping variations in the cuprates.[43] However, a recent tunneling experiment on YBCO suggests that the pairing symmetry may evolve under field-induced supercurrents.[44] Further current-dependent studies, in conjunction with doping variation, would be needed to elucidate this issue.

We note that ZBCP were also seen on {001} samples, showing the same suppression effect by currents applied predominantly along <100>. Figure 4 plots an example of such ZBCP at 4.2K. Such ZBCP have previously been observed on c-axis cuprate thin films,[45] and could be explained by the presence of terrace edges on the film surface (see inset of Fig.5) which would allow in-plane tunneling to occur on nominally c-axis samples. The probability for in-plane tunneling could also be enhanced by the inherently larger matrix element for in-plane

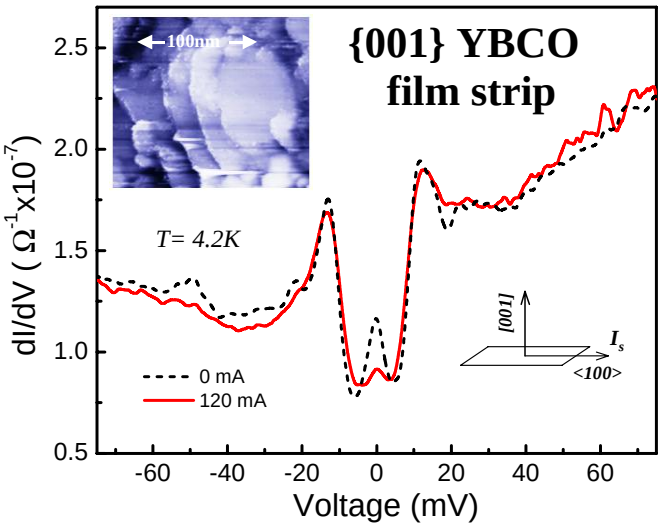

Figure 5. *dI/dV* spectra obtained on a {001} YBCO thin-film strip carrying a supercurrent applied predominantly along <100> at 4.2K. The inset shows typical film topography imaged by STM.

versus *c*-axis tunneling.[46] Consistent with this picture are instances where the ZBCP is seen together with a gap structure at the same tip location on {001} samples. The main panel in Fig.5 shows such a spectrum, with a midgap peak flanked by well-developed gap edges at $\approx\pm$14meV. The gap structures could be identified as the *d*-wave averaged density of states associated with *c*-axis tunneling.[13,46] Since *c*-axis tunneling does not involve Andreev interference, the gap structures are expected to depend only on the OP amplitude and be relatively insensitive to the OP phase fluctuations. What we observe in Fig.5 is entirely consistent with this expectation. Upon the application of a supercurrent, the ZBCP is suppressed as before but without significant variation in the gap structure. This is a remarkable observation, indicating that a sub-critical current can weaken the local phase coherence while maintaining the pairing amplitude. This "dephasing-without-depairing" scenario can be viewed essentially as a pseudogap-like condition at short spatial ranges, despite the preservation of long-range phase coherence. These results suggest that the pseudogap state is perhaps not merely a *thermodynamic* phenomenon, but could also be *electrodynamically* nucleated at coherence-length scales.

In summary, using a novel scanning tunneling spectroscopy technique we have observed nanoscale suppression of low-energy Andreev states by a directly-applied supercurrent in $YBa_2Cu_3O_{6+x}$ thin-film strips at 4.2K. This suppression effect can be interpreted within the *d*-wave BTK formalism as evidence for order-parameter dephasing at coherence-length scales. Our results indicate that a *static* phase gradient can *dynamically* disturb the *local* phase order, thus implicating phase fluctuations in the phenomenon of high-temperature superconductivity.

3. CURRENT-DRIVEN PHASE SLIPS IN YBCO MICROWIRES

The dissipative processes which give rise to resistance in superconducting thin films are essentially local in nature. In wide films, resistance occurs due to the motion of magnetic vortices induced by an applied current. In narrow films, where the width w is less than the superconducting coherence length ξ and vortices cannot readily form, resistance is generally due to the occurrence of phase slips. Phase slips are a fundamental effect of fluctuations in the superconducting order parameter (OP).[3,4,47] Such fluctuations can either be thermally activated[48] or proceed by macroscopic quantum tunneling,[49–52] both producing measurable resistance. Phase slips can also occur under a large applied current,[3] essentially as a *dynamic* response of the superconducting OP to a *static* phase gradient.[53] In the current-driven phase slip process, the OP undergoes an AC Josephson-like oscillation within a region known as a phase slip center (PSC), which is $\sim 2\xi$ in length. Whenever the OP crosses zero, its phase slips by 2π. This phase slippage allows for local dissipation while preserving global phase coherence through a relaxation of the superfluid momentum.[54]

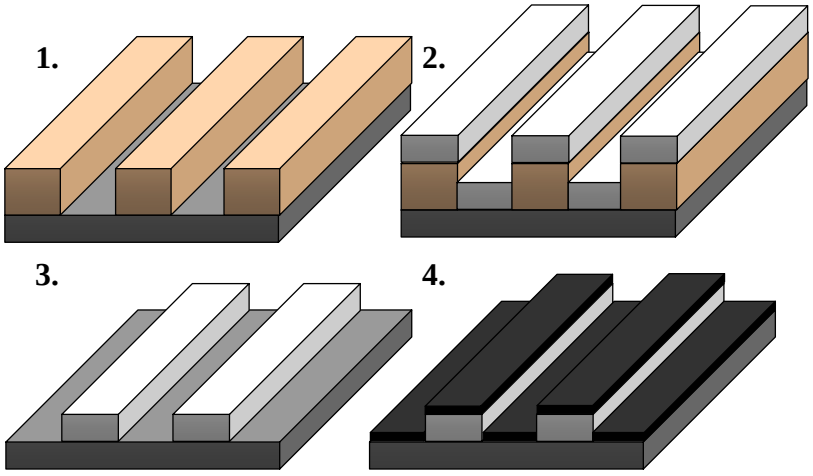

Figure 6. Nanofabrication Technique: 1. A PMMA mask is defined using electron-beam lithography. 2. A layer of amorphous STO is deposited by PLD at ambient temperature. 3. The PMMA mask is removed leaving amorphous STO barriers. 4. A YBCO thin film is deposited by PLD on the patterned substrate.

Recent advances in nanotechnology have enabled current-driven phase slips to be studied in very narrow samples. For conventional low-T_c superconductors, these studies are usually carried out in quasi-1D nanowires, with $w<\xi$, to show distinctive current-voltage (I-V) nonlinearities which can be related to phase-slip dissipation.[55] These I-V measurements have tended to be made under *current*-biasing and close to the critical temperature. More recently, phase slip studies have been extended to quasi-2D geometries ($w>\xi$), which have shown similar I-V nonlinearities, thus demonstrating the formation of phase slip lines (PSL)..[56–59] As a quasi-2D analogue of PSCs, the spatially-extended PSLs had been theoretically predicted, based on the existence of kinematic vortices.[57,60] For the high-T_c superconductors, the study of electrically-driven phase slips has generally been limited by their high critical-current densities, short coherence lengths, and inherent chemical sensitivity.[5] Nevertheless, several transport studies have been reported on chemically- or physically-etched cuprate thin films, ranging from 100nm to 20μm in width.[32,33,61–65] In these studies, highly nonlinear I-V characteristics were seen below T_c, and attributed to either collective flux flow, vortex instability, mesoscopic domains or phase slip regions.

Here we report I-V characteristics of *optimally-doped* $YBa_2Cu_3O_{7-\delta}$ (YBCO) microwires which were fabricated by a *chemical-free* method. The microwires were measured under both *current*- and *voltage*-biasing. A pulsed-signal technique was used to eliminate Joule heating and enabled measurement down to 4.2K. Anomalous S-shaped nonlinearities were observed under *voltage*-biasing, in striking agreement with the phase slip phenomenology established in Ref.[66,67] for low-T_c superconductors in quasi-1D geometries. We interpret this observation as evidence for the formation of current-driven PSLs in our quasi-2D high-T_c microwires.

3.1. Nanofabrication

Optimally-doped YBCO microwires were fabricated using a chemical-free technique based on selective epitaxial growth,[34] whereby the epitaxial growth of YBCO is limited to select regions by the presence of amorphous STO barriers. The STO barriers act to electrically and physically isolate select regions of the YBCO film, and their amorphous nature ensures that the YBCO deposited on top of the barriers will be of poor crystallinity and hence poor conductivity. Surface images of the YBCO deposited on top of the STO barriers, taken by atomic force microscopy (AFM), confirmed their amorphous nature, and resistance versus temperature measurements confirmed their insulating behavior.

The initial stage of the fabrication process involves defining a polymethylmethacrylate (PPMA) mask on a single crystal STO substrate by electron-beam lithography. A layer of amorphous STO is then deposited on the

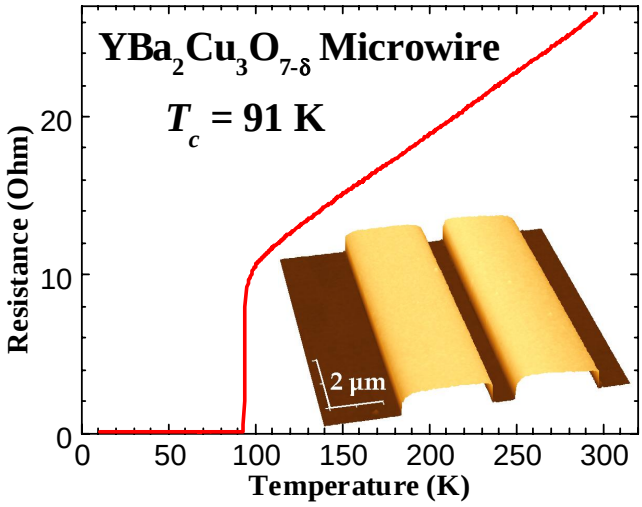

Figure 7. Resistance versus temperature for an optimally-doped YBCO microwire 1.00μm wide and 80μm long. Inset shows a perspective AFM image of a typical YBCO microwire, with the light regions being the amorphous barriers and middle dark region being the epitaxial channel.

substrate by pulsed laser-ablated deposition (PLD). The deposition of the STO is done at ambient temperature to ensure the amorphous nature of the deposited STO. Immersing the substrate in acetone in an ultrasonic bath removes the PMMA mask leaving behind the amorphous STO barriers. A thin film of YBCO is then deposited on the patterned substrate using typical deposition conditions. Epitaxial growth of the deposited YBCO will only occur on regions of the substrate devoid of amorphous STO. Since the deposition of YBCO is the last stage of the fabrication process and no chemical or physical etchants come in contact with the deposited YBCO, its integrity is preserved. YBCO microwires fabricated using this technique were typically 1 μm wide x 100 μm long (in the *ab*-plane) and 50 nm thick (along the *c*-axis). Resistance versus temperature measurements of the microwires exhibit sharp superconducting transitions at $\approx$ 91K, which is typical of unpatterned films.

3.2. Pulsed $I-V$ Measurements

The *I*-*V* characteristics of YBCO microwires were measured both as a function of current $V(I)$ and as a function of voltage $I(V)$. Pulsed signals were used to minimize Joule heating which could result from the inherently large current densities associated with high-T_c superconductors. For both *current*-biased and *voltage*-biased modes, 200 μs pulses with duty cycles of 5% were used. Data is averaged over the final 170 μs of each pulse to reduce any transient effects and averaged over 50 pulses to provide an adequate signal-to-noise ratio.

Typical *I*-*V* characteristics of our microwires in both *current*-biased and *voltage*-biased modes are shown in Figure 8. A distinct discontinuity is observable in the $V(I)$ data above a threshold value of applied current (I^*). For sufficiently low temperatures, below I^*, the *I*-*V* characteristic is linear. As the temperature of the sample increases, the *I*-*V* characteristic of the microwire below I^* can be described by a power law relation, as indicated in the inset, suggesting that the dissipation in the microwire is due to flux flow. Above each discontinuity, the $V(I)$ becomes linear. The threshold value of current I^* expectedly decreases as the temperature of the microwire increases. In the $I(V)$ curves shown in Figure 8, anomalous *S*-shaped nonlinearities are seen. Above a threshold value of the applied voltage (V^*) in each curve, the current through the microwire decreases. A second threshold value of the voltage is also present, above which the current through the microwire increases as the voltage increases and the *I*-*V* curve becomes linear. At each temperature measured, the discontinuity in the $V(I)$ coincides with the *S*-shaped nonlinearity in the $I(V)$.

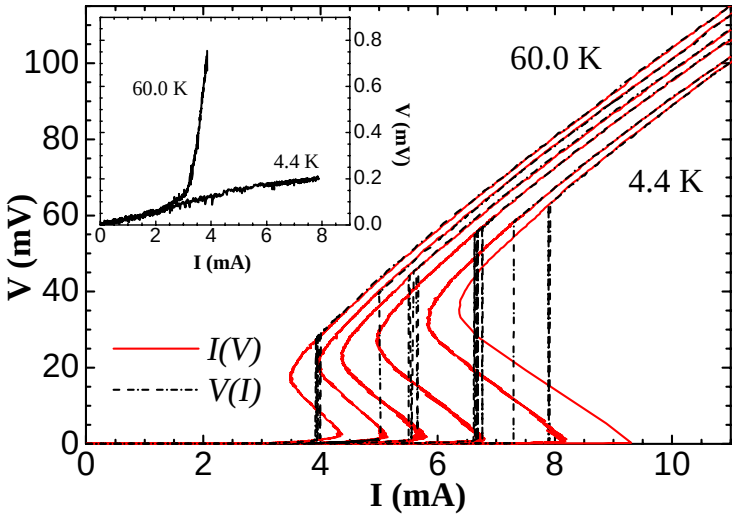

Figure 8. Current-voltage characteristics of an optimally-doped YBCO microwire 1μm wide and 80μm long. Data shown was taken at 4.4, 30.0, 42.5, 50.0, 55.0 and 60.0 K, under both *current*-biasing (dashed) and *voltage*-biasing (solid). Inset shows $V(I)$ for the same microwire at 4.4 and 60.0 K for values of applied current less than I^*.

3.3. Phase Slip Analysis

Our I-V data bear striking resemblance to the data reported on quasi-1D superconducting Pb and Sn nanowires in Ref..[66] In this earlier work, S-shaped $I(V)$ nonlinearities which coincide with the $V(I)$ discontinuities were attributed to the formation of PSCs in the nanowires. In the *current*-biased mode, the $V(I)$ jumps abruptly at I^* as a PSC is formed along the nanowire. Non-equilibrium quasiparticles resulting from the OP fluctuation within this PSC would diffuse over a distance $\Lambda_Q(T)$ on either side before recombining into the condensate.[68] This region is responsible for the increment of ohmic resistance in the microwire, corresponding to the linear segment of the I-V curve above I^*. Under *voltage*-biasing, the coinciding S-shaped nonlinearities are explained in terms of the dynamics of phase-slip metastability using a time-dependent Ginzburg-Landau (TDGL) formalism.[66,67] According to Ref.,[67] the condition for the occurrence of PSCs is determined by the competition between two relaxation times scales: τ_ϕ which corresponds to the OP phase; $\tau_{|\psi|}$ which corresponds to the OP amplitude. A PSC will occur in a superconducting nanowire if $\tau_\phi < \tau_{|\psi|}$. In essence, the S-shaped nonlinearities seen under *voltage*-biasing can be identified as a distinct signature for the formation of PSCs, which have traditionally been associated with the step structures seen in *current*-biased data.[3] And the observation of similar S-shaped nonlinearities in our quasi-2D YBCO microwires implies the formation of spatially-extended PSLs.

3.4. Results and Discussion

The experimental evidence we observed for the formation of PSLs in YBCO microwires has important implications for the study of high-T_c superconductivity. First, the appearance of S-shaped nonlinearities is consistent with a characteristically short phase-relaxation timescale corresponding to τ_ϕ.[66,67] Because high-T_c cuprates have low carrier densities and thus low superfluid rigidity, they are inherently prone to phase fluctuations[6] which would make them more susceptible to phase slips in reduced dimensions than conventional low-T_c superconductors. We are currently examining this issue further through a doping-dependent study of phase slips in the cuprates. Second, the appearance of the anomalous I-V nonlinearities in our microwires indicates that such phase non-equilibrium tends to occur at very short length scales, consistent with the STM spectroscopy study of *current-driven* YBCO thin films discussed above in Section 2. This length-scale dependence could offer important clues on the origin of the pseudogap state.[10] Third, it is distinctly possible that coexisting quantum-ordered states, such as spin/charge stripes,[30] spin-density waves[35] or staggered-flux like states[36,37,69] could provide natural topological weak links for the nucleation of phase slips to produce distinctive I-V nonlinearities. In this

connection, we note that in our experiment strips wider than ∼2um showed no such nonlinearities, indicating that the stable formation PSL's in YBCO may require some degree of spatial confinement transverse to the supercurrent.

4. SUMMARY AND CONCLUSION

In summary, we have developed two new *nanoscale* techniques for probing high-T_c cuprates superconductors in the *current-carrying* state. These techniques represent complementary "bottom-up" and "top-down" approaches to the study of short-range phase dynamics in cuprate superconductors. First, taking advantage of the phase sensitivity of *d*-wave Andreev interference, scanning tunneling spectroscopy was used to reveal distinct evidence for current-driven dephasing at the coherence-length scale in YBCO thin films. Second, by careful measurement and analysis of the nonlinear *I-V* characteristics in nanostructured YBCO microwires, we have observed robust signatures of current-driven phase slip lines. These phenomena represent profound *dynamic* responses of cuprate superconductors to a *static* phase gradient, and reveal an inherent phase *non-rigidity* of the high-T_c order parameter under electrodynamic perturbation. Our results have specific significance for the understanding high-T_c superconductivity, and could also shed general light on the fundamental relationship between vortex fluctuations and phase slippage in reduced dimensions.

ACKNOWLEDGMENTS

This work is supported by NSERC, CFI/OIT, MMO/EMK and the Canadian Institute for Advanced Research. The authors gratefully acknowledge research assistance from Massimo DiCiano, Eugenia Tam, Stephanie Chiu, Liz Chia-Wei Chang and Jonathan Grzymisch.

REFERENCES

1. K. Epstein, A. M. Goldman and A. M. Kadin, "Vortex-Antivortex Pair Dissociation in Two-Dimensional Superconductors," *Phys. Rev. Lett.* **47**, pp. 534-537, 1981.
2. M. R. Beasley, J. E. Mooij and T. P. Orlando, "Possibility of Vortex-Antivortex Pair Dissociation in Two-Dimensional Superconductors," *Phys. Rev. Lett.* **42**, pp. 1165-1168, 1979.
3. W.J. Skocpol, M.R. Beasley and M. Tinkham, "Phase-slip centers and nonequilibrium processes in superconducting tin microbridges," *J. Low. Temp. Phys* **16**, p.145, 1974.
4. B.I. Ivlev and N.B. Kopnin, "Electric currents and resistive states in thin superconductors," *Advs. in Phys.*, **33**, p.47, 1984.
5. I. Bozovic *et al.*, "Atomic-layer engineering of cuprate superconductors", *J. Supercond.* **7**, pp. 187-195, 1994.
6. V. J. Emery and S. A. Kivelson, "Importance of phase fluctuations in superconductors with small superfluid density", *Nature* **374**, pp. 434-437, 1995; V. J. Emery and S. A. Kivelson, "Superconductivity in Bad Metals," *Phys. Rev. Lett.* **74**, pp. 3253-3256, 1995; E. W. Carlson, S. A. Kivelson, V. J. Emery, and E. Manousakis, "Classical Phase Fluctuations in High Temperature Superconductors" *Phys. Rev. Lett.* **83**, 612 (1999).
7. L. Merchant *et al.*, "Crossover from phase fluctuation to amplitude-dominated superconductivity: A model system," *Phys. Rev. B* **63**, pp. 134508-134513, 2001.
8. For example, see Y. J. Uemura, in *Proceedings of the CCAST Symposium, Beijing, 1994*, S. Feng and H. C. Ren, ed., Gordon and Breach, New York, pp. 113-142, 1995.
9. For a review, see M. Randeria, "Crossover from BCS Theory to Bose-Einstein Condensation," in *Bose-Einstein Condensation*, A. Griffin, D. Snoke and S. Stringari, ed., Cambridge University Press, Cambridge, 1995.
10. For a review, see T. Timusk and B. Statt, "The pseudogap in high-temperature superconductors: an experimental survey," *Rep. Prog. Phys.* **62**, pp. 61-122, 1999.
11. C.-R. Hu, "Midgap surface states as a novel signature for $d_{x^2-y^2}$-wave superconductivity," *Phys. Rev. Lett.* **72**, pp. 1526-1529, 1994.
12. Y. Tanaka and S. Kashiwaya, "Theory of Tunneling Spectroscopy of d-Wave Superconductors," *Phys. Rev. Lett.* **74**, pp. 3451-3454, 1995.

13. J. Y.T. Wei *et al.*, "Directional Tunneling and Andreev Reflection on $YBa_2Cu_3O_{7-\delta}$ Single Crystals: Predominance of d-Wave Pairing Symmetry Verified with the Generalized Blonder, Tinkham, and Klapwijk Theory," *Phys. Rev. Lett.* **81**, pp. 2542-2545, 1998.
14. For a recent review, see G. Deutscher, "Andreev—Saint-James reflections: A probe of cuprate superconductors," *Rev. Mod. Phys.* **77**, pp. 109-135, 2005.
15. J. Ngai *et al.*, "Scanning tunneling spectroscopy under pulsed spin-injection," *Appl. Phys. Lett.* **84**, p. 1908-1910, 2004.
16. T. Frey, C.C. Chi, C.C. Tsuei, T. Shaw, and F. Bozso, "Effect of atomic oxygen on the initila growth mode in thin epitaxial cuprate films,", *Phys. Rev. B* **49**, p. 3483, 1994.
17. D. Zhang, C. S. Ting, and C.-R. Hu, "Conductance characteristics between a normal metal and a clean superconductor carrying a supercurrent," *Phys. Rev. B* **70**, pp. 172508-172511, 2004.
18. M. Aprili, E. Badica, and L.H. Greene, "Doppler Shift of the Andreev Bound States at the YBCO Surface," *Phys. Rev. Lett.* **83**, pp. 4630-4633, 1999, and references therein.
19. H.-Y. Choi, Y. Bang and D.K. Campbell, "Andreev reflections in the pseudogap state of cuprate superconductors," *Phys. Rev. B* **61**, pp. 9748-9751, 2000.
20. M. Franz and A. J. Millis, "Phase fluctuations and spectral properties of underdoped cuprates," *Phys. Rev. B* **58**, pp. 14572-14580, 1998.
21. K. V. Samokhin and M. B. Walker, "Localized surface states in high-temperature superconductors: Alternative mechanism of zero-bias conductance peaks," *Phys. Rev. B* **64**, pp. 172506-172509, 2001.
22. K. V. Samokhin, "Impurity resonances in the mixed state of high-Tc superconductors," *Phys. Rev. B* **68**, pp. 104509-104512, 2003.
23. J. X. Zhu *et al.*, "Quasiparticle resonant states induced by a unitary impurity in a d-wave superconductor," *Phys. Rev. B* **61**, pp. 8667-8670, 2000.
24. I. Adagideli *et al.*, "Low-Energy Quasiparticle States near Extended Scatterers in d-Wave Superconductors and Their Connection with SUSY Quantum Mechanics," *Phys. Rev. Lett.* **83**, pp. 5571-5574, 1999.
25. Y. Tanuma *et al.*, "Local density of states on rough surfaces of $d_{x^2-y^2}$-wave superconductors," *Phys. Rev. B* **57**, pp. 7997-8008, 1998.
26. A. V. Balatsky, M. I. Salkola, and A. Rosengren, "Impurity-induced virtual bound states in d-wave superconductors," *Phys. Rev. B* **51**, pp. 15547-15551, 1995.
27. D. Zhang, C. S. Ting, and C.-R. Hu, "Impurity-induced local density of states in a d-wave superconductor carrying a supercurrent," *Phys. Rev. B* **71**, pp. 064521-064527, 2005.
28. P. Minnhagen, "The two-dimensional Coulomb gas, vortex unbinding, and superfluid-superconducting films," *Rev. Mod. Phys.* **59**, pp. 1001-1066, 1987.
29. Z. Tesanovic, O. Vafek, and M. Franz, "Chiral symmetry breaking and phase fluctuations: A QED3 theory of the pseudogap state in cuprate superconductors," *Phys. Rev. B* **65**, pp. 180511(R)-180514, 2002.
30. For a review on stripe phenomenology, see S. A. Kivelson *et al.*, "How to detect fluctuating stripes in the high-temperature superconductors," *Rev. Mod. Phys.* **75**, pp. 1201-1241, 2003.
31. A. H. Castro Neto, "Superconducting Phase Coherence in Striped Cuprates," *Phys. Rev. Lett.* **78**, pp. 3931-3934, 1997.
32. J. A. Bonetti *et al.*, "Electronic Transport in Underdoped $YBa_2Cu_3O_7$ Nanowires: Evidence for Fluctuating Domain Structures," *Phys. Rev. Lett.* **93**, pp. 087002-087005, 2004.
33. F.S. Jelila *et al.*, "Time of Nucleation of Phase-Slip Centers in $YBa_2Cu_3O_7$ Superconducting Bridges," *Phys. Rev. Lett.* **81**, pp. 1933-1936, 1998.
34. P. Morales, M. DiCiano and J.Y.T. Wei, "Selective epitaxial growth of submicron complex oxide structures by amorphous $SrTiO_3$", *Appl. Phys. Lett.*, **86**, p. 192509, 2005.
35. E. Demler, S. Sachdev, and Y. Zhang, "Spin-Ordering Quantum Transitions of Superconductors in a Magnetic Field," *Phys. Rev. Lett.* **87**, pp. 067202-067205, 2001.
36. J. B. Marston and I. Affleck, "Large-n limit of the Hubbard-Heisenberg model," *Phys. Rev. B* **39**, pp. 11538-11558, 1989.
37. S. Chakravarty *et al.*, "Hidden order in the cuprates," *Phys. Rev. B* **63**, pp. 094503-094513, 2001.

38. Y. B. Kim and X. G. Wen, "Effects of collective modes on pair tunneling into superconductors," *Phys. Rev. B* **48**, pp. 6319-6329, 1993.
39. P. Devillard *et al.*, "Andreev reflection off a fluctuating superconductor in the absence of equilibrium," *Phys. Rev. B* **66**, pp. 165413-165423, 2002.
40. I. Khavkine, H.-Y. Kee, and K. Maki, "Supercurrent in Nodal Superconductors", *Phys. Rev. B* **70**, pp. 184521-184525, 2004.
41. M. Zapotocky, D. L. Maslov and P. M. Goldbart, "Induction of non-d-wave order-parameter components by currents in d-wave superconductors," *Phys. Rev. B* **55**, pp. 6599-6604, 1997.
42. V. V. Kabanov, "Zeros of the order parameter of $d_{x^2-y^2}$ superconducting film in the presence of uniform current," *Phys. Rev. B* **69**, pp. 052503-052505, 2004.
43. C. C. Tsuei *et al.*, "Robust $d_{x^2-y^2}$ Pairing Symmetry in Hole-Doped Cuprate Superconductors," *Phys. Rev. Lett.* **93**, pp. 187004-187007, 2004.
44. R. Beck *et al.*, "Remarkable change of tunneling conductance in YBCO films in fields up to 32.4T," cond-mat/0407199.
45. S. Misra *et al.*, "Formation of an Andreev bound state at the step edges of $Bi_2Sr_2CaCu_2O_8$ surface," *Phys. Rev. B* **66**, pp. 100510(R)-100513, 2002.
46. J. Y.T. Wei *et al.*, "Quasiparticle tunneling spectra of the high-T_c mercury cuprates: Implications of the d-wave two-dimensional van Hove scenario," *Phys. Rev. B* **57**, pp. 3650-3662, 1998.
47. M. Tinkham, *Introduction to Superconductivity*, McGraw-Hill, New York, 1996.
48. J.S. Langer and V. Ambegaokar, "Intrinsic resistive transition in narrow superconducting channels," *Phys. Rev.*, **164**, pp. 498-510, 1967; D.E. McCumber and B.I. Halperin, "Time scale of intrinsic resistive fluctuations in thin superconducting wires", *Phys. Rev. B*, **1**, pp. 1054-1070, 1970.
49. N. Giordano, "Evidence for macroscopic quantum tunneling in one-dimensional superconductors," *Phys. Rev. Lett.*, **61**, pp. 2137-2140, 1988.
50. P. Xiong, A. V. Herzog, and R. C. Dynes, "Negative Magnetoresistance in Homogeneous Amorphous Superconducting Pb Wires," *Phys. Rev. Lett.* **78**, 927 (1997); A. V. Herzog et al., **76**, 668 (1996).
51. A. Bezryadin *et al.*, "Quantum suppression of superconductivity in ultrathin nanowires," *Nature* **404**, pp. 971 - 974, 2000; C. N. Lau *et al.*, "Quantum phase slips in superconducting nanowire," *Phys. Rev. Lett.*, **87**, p. 217003, 2001.
52. A.D. Zaikin *et al.*, "Quantum Phase Slips and Transport in Ultrathin Superconducting Wires," *Phys. Rev. Lett.*, **78**, pp. 1552-1555, 1997.
53. L. Krammer and A. Baratoff, "Lossless and dissipative current-carrying states in quasi-one-dimensional superconductors," *Phys. Rev. Lett.*, **38**, pp. 518-521, 1977.
54. P.W. Anderson and A. Dayem, "Radio-frequency effects in superconducting thin film bridges," *Phys. Rev. Lett.*, **13**, pp. 195-197, 1964.; P.W. Anderson, "Considerations on flow of superfluid helium," *Rev. Mod. Phys.* **38**, pp. 298-310, 1966.
55. M. L. Tian *et al.*, "Dissipation in quasi-one-dimensional superconducting single-crystal Sn nanowires," *Phys. Rev. B.*, **71**, p. 104521, 2005.
56. I.M. Dmitrenko, "Resistive state of wide superconducting films and phase slip lines (Review)," *Low Temp. Phys.* **22**, pp. 648-869, 1996.
57. V.G. Volotskaya *et al.*, "Current-induced destruction of superconductivity in wide films," *Fiz. Nizk. Temp.* **7**, pp. 383-386, 1981 [*Sov. J. Low Temp. Phys.* **7**, pp. 188-191, 1981.]
58. A.G. Sivakov *et al.*, "Josephson behavior of phase-slip lines in wide superconducting strips," *Phys. Rev. Lett.*, **91**, p. 267001, 2003.
59. V.M. Dmitriev *et al.*, "Critical currents, phase slip centers, and phase slip lines in superconducting films in the absence of external magnetic field," *Low Temp. Phys.* **31**, pp. 127-136, 2005.
60. A. Andronov et al., "Kinematic vortices and phase slip lines in the dynamics of the resistive state of narrow superconductive thin film channels," *Physica C* **213**, 193, (1993). The kinematic vortices have characters intermediate between Abrikosov and Josephson vortices, and are essentially topological carriers of OP singularities in phase slip lines.

61. M.J.M.E. de Nivelle *et al.*, "Thermally activated coherent vortex motion in $YBa_2Cu_3O_7$ thin film microbridges," *Phys. Rev. Lett.*, **70**, pp. 1525-1528, 1993.
62. V.M. Dmitriev *et al.*, "Phase-slip processes induced by microwave field and direct current in superconducting ceramic $YBa_2Cu_3O_{7-x}$," *Physica C*, **235-240**, pp. 1973-1974, 1994.
63. M.M. Abdelhadi and J.A. Jung, "Phase-slip-like resistivity in underdoped $YBa_2Cu_3O_7$," *Phys. Rev. B*, **67**, p. 054502, 2003.
64. S.G. Doettinger *et al.*, "Electronic instability at high flux-flow velocities in high-Tc superconducting films," *Phys. Rev. Lett.*, **73**, pp. 1691-1694, 1994.
65. M.N. Kunchur, "Unstable flux flow due to heated electrons in superconducting films," *Phys. Rev. Lett.*, **89**, p. 137005, 2002.
66. D.Y. Vodolazov *et al.*, "Current-voltage characteristics of quasi-one-dimensional superconductors: An S-shaped curve in the constant voltage regime," *Phys. Rev. Lett.*, **91**, p. 157001, 2003.
67. S. Michotte *et al.*, "Condition for the occurrence of phase slip centers in superconducting nanowires under applied current or voltage," *Phys. Rev. B*, **69**, p. 094512, 2004.
68. A.B. Pippard *et al.*, "Resistance of superconducting-normal interfaces," *Proc. Roy. Soc*, **A324**, p. 17, 1971.
69. C.M. Varma, "Non-Fermi-liquid states and pairing instability of a general model of copper oxide metals," *Phys. Rev. B*, **55**, pp. 14554-14580, 1997.